Available online at www.sciencedirect.com
ScienceDirect
Composite Structures 82 (2008) 475–487
COMPOSITE STRUCTURES
www.elsevier.com/locate/compstruct

Seismic retrofit of reinforced concrete short columns by CFRP materials

F. Colomb [a], H. Tobbi [b], E. Ferrier [b,*], P. Hamelin [b]

[a] GTM Construction, DITC, 61 Av, Jules Quentin, 92730 Nanterre cedex, France
[b] LGCIE, Université de Lyon, Université Lyon 1, INSA-LYON, 82 bd Niels Bohr, F-69622 Villeurbanne, France

Available online 4 February 2007

Abstract

Nowadays, reinforcing buildings or bridges against earthquake damage is a real technico-economic challenge. Composite materials applied by the wet lay-up method have been the main reinforcement technology for civil engineering structures since the 1990s. The research developed in this paper concerns seismic reinforcement. The main objectives are to evaluate CFRP's contribution to mechanical and energetic performance and to the modification of the cracking pattern on short columns. During earthquakes, short columns undergo shear stress due to their low resistance to high imposed horizontal displacements.

Eight short columns were tested; their longitudinal reinforcement was higher than the Eurocode 8 upper limit whereas transverse reinforcement was insufficient, in order to ensure shear failure. Seven were continuously or discontinuously reinforced by CFRP or GFRP. They were tested under a constant compression load combined with a horizontal quasi-static cyclic load. It was therefore possible to evaluate the efficiency of such reinforcement by measuring the gain in terms of load and ductility.

Keywords: Short columns; Seismic retrofit; CFRP

1. Introduction

Making existing reinforced concrete buildings and prestressed concrete constructions conform to safety regulations and considerations regarding accidents such as earthquakes and explosions is a great technological and financial challenge which poses a huge socio-economic problem for the years to come [1]. Examination of existing engineering structures brings to light initial design errors and/or material degradation needing new methods of reinforcement or repair. In the last decade, composite materials (carbon or glass fibres associated with polymeric matrices) applied by bonding have proved their effectiveness in the protection and reinforcement of beams and columns [2].

Civil engineering structures as well as office or apartment buildings are affected by earthquakes. A common cause of failure seems to be shear stress. It appears mainly for columns having a weak slenderness. It is characterised by a diagonal brittle fracture of the elements in reinforced concrete [3]. Composite material reinforcement against shear effects is well-known and used by the large civil engineering companies (e.g. on the sides of beams). The effectiveness of reinforcement in our particular case is already proven. The aim of this paper is to determine whether composite materials can be used in seismic reinforcement, particularly for short columns.

Retrofitting reinforced concrete structures generally requires additional material, or more rarely, additional loads [4]; in the case of seismic reinforcement, the usual techniques in the category "additional material" are:

- Reinforced concrete jacketing.
- Steel jacket.
- Steel plates bonding.

Over the last decade, and especially since the Northridge (1994), Kobe (1995) and Taiwan (1999) earthquakes [1,3,5], strengthening with composite materials has become more common.

* Corresponding author. Tel.: +33 472 692 130; fax: +33 478 94 69 06.
E-mail address: Emmanuel.Ferrier@univ-lyon1.fr (E. Ferrier).

0263-8223/$ - see front matter © 2007 Elsevier Ltd. All rights reserved.
doi:10.1016/j.compstruct.2007.01.028

1.1. Shear failure

This type of failure is brittle and non-dissipative. It is characterized by diagonal cracks in the concrete (as soon as the tensile stress of the concrete is reached), then transverse reinforcement yields followed by the buckling of the longitudinal rebar, at which stage the concrete is completely crushed [6]. Care must be taken to avoid this failure mode [6,7]. Shear failure appears when the transverse reinforcement is insufficient. It is frequent in short columns (Fig. 1). We would underline that short columns can have a structural origin (e.g. underground, with openings of low height, under-floor spaces, etc.). Short columns can also result from structural modifications: the original columns being shortened by the installation of barges or partial masonry, symmetrically or not [3].

1.2. Seismic reinforcement

Whatever the reinforcement method, the seismic reinforcement strategy of a structure generally has three aims:

- Enhancement of load-bearing capacity.
- Enhancement of strength and ductility.
- Increase in ductility.

The choice of strategy depends on the category of the structure, but seismic reinforcement of the reinforced concrete posts always consists of increasing the ductility, for the more ductile the behaviour, the more it dissipates the energy induced by the seismic load, preventing non-dissipative (brittle) failure, which civil engineers generally try to avoid [3]. The choice of strengthening to increase the ductility rather than the load-bearing capacity is explained by the fact that this involves an increase in seismic load and a reduction in post-elastic deformation. This reinforcement is necessary when there is insufficient longitudinal reinforcement due to design error or rebar corrosion. Fig. 2 shows the behaviour of a structural element which has been strengthened for resistance and/or ductility in accordance with criteria for the seismic safety of buildings [8,9]. It seems clear that to obtain the same level of energy dissipation, the strength enhancement strategy requires a significant increase in strength (×3 or ×4) and consumes more materials; reinforcement in ductility is therefore preferable [10].

Several studies [11–13] on the effect of external bonded FRP reinforcement on the shear behaviour of strengthened short columns have already been done. The experimental work done enhance the fact that the continuous FRP reinforcement column wrapping allows to increase the ultimate displacement and the ultimate strength. If all the results are interesting, there still exist a need to increase the data base of CFRP strengthened short column loaded in shear. It would thus be useful to know how the composite sheet wrapping enhances the ductility. The aim of this study is to evaluate the increase in strength and in ductility resulting from the use of FRP depending on the FRP reinforcement ratio, the FRP reinforcement position (continuous or partial) and the material properties (Young modulus, ultimate strength.

1.3. FRP shear reinforcement of columns

Based on some experimental work found in the literature dealing with short RC column seismic retrofitting [14], we undertook an experimental programme. In this work, several parameters were studied, the most significant being the shear span to depth ratio (a/h), the configuration

Fig. 1. Shear rupture of the piles *Hanshin-Awaji seism* [8].

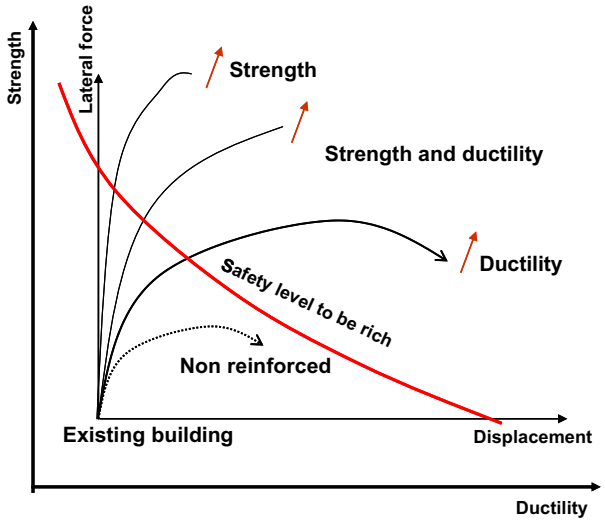

Fig. 2. Reinforcement strategy [4].

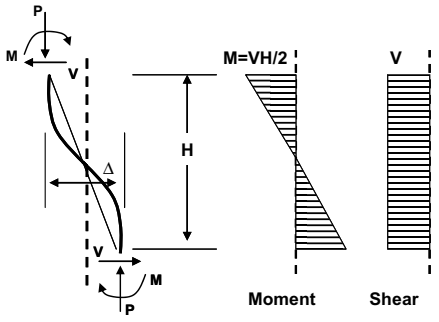

Fig. 3. Double curvature loading.

of the composite (thickness and partial or full wrapping of the column) and the intensity of axial loading.

The importance of the shear span to depth ratio is due to the fact that the smaller this ratio is, the more the bending moment is reduced; as the shear stress remains the same, the result is shear failure. The bending moment becomes minimal for boundary conditions (fixed–fixed). With a horizontal force applied at the middle height of the column, the point of inflection (null bending moment) is also in the middle of the column. The displacement resulting from this test configuration is known to be a double curve (double curvature or double bending) as shown in Fig. 3. Shear stress is constant all along the column and bending is maximal at the top and the bottom of the column.

The longitudinal reinforcement ratio (ρs) has been taken equal to the maximum authorised percentage which is $\rho_s = 4\%$ [15], while the transverse reinforcement ratio (ρ_t) is equal to the minimum percentage of the old French rules [16] $\rho_t = 0.14\%$.

2. Experimental procedure

2.1. Materials of reinforcement

The reinforcement is applied by the wet lay-up method in the ROCC® process. The mechanical properties of the fabric, resin and composite are summarised in Tables 1–3.

Table 1
Properties of fabric

One way carbon fabric	
Weight (g/m^2)	622
Tensile strength (MPa)	4000
Tensile modulus (MPa)	240000
Ultimate strain (%)	1.60

Table 2
Properties of the resin

Epoxy resin	
Tensile strength (MPa)	56
Tensile modulus (MPa)	3200
Ultimate strain (%)	2.3
Glass transition temperature (°C)	56

Table 3
Properties of the CFRP

Composite ROCC®	
Tensile strength (MPa)	880
Tensile modulus (MPa)	80000
Ultimate strain (%)	1.1

2.2. Specimens design

The columns have a square section of 200 mm × 200 mm^2, which is a 2/3 scale of real short columns in buildings. These specimen sizes were selected as being representative of reality. The selected slenderness is equal to three ($H/L = 3$), which finally gives columns of 200 mm × 200 mm × 600 mm. A slenderness of 3 is the upper limit of the short column notion. Eight 16 mm steel rebars are used for the longitudinal reinforcement and three 6 mm frames separated by 200 mm for transverse reinforcement. In order to reproduce the boundary conditions as accurately as possible, the columns were embedded at their two ends in two reinforced concrete blocks of 600 × 600 × 300 mm^3 to avoid failure in the embeddings. Fig. 4 shows the specimen dimensions. Fig. 5 describes the reinforcement.

The set of eight columns may be described as follows (one was not reinforced (SC-1) and will be used as a reference). For the seven remaining columns, the parameters taken into account were the thickness of the FRP reinforcement (numbers of layers) and its configuration. The second column was reinforced by carbon layers of 100 mm in width, 100 mm apart (SC-PW-2C 1). The third and fourth columns were reinforced on the entire height by, respectively, two and three layers of carbon FRP (columns SC-FW-2C and SC-FW-3C). In order to optimise the reinforcement, the remaining columns were partially wrapped,

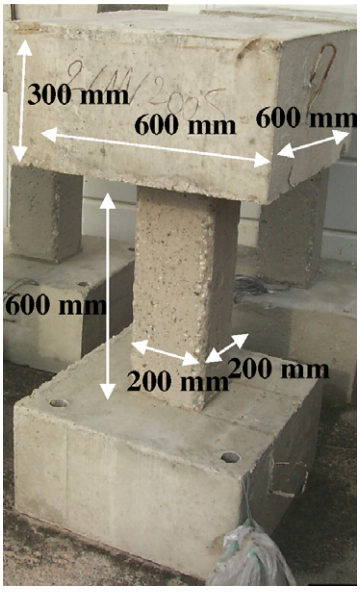

Fig. 4. Description of the specimens.

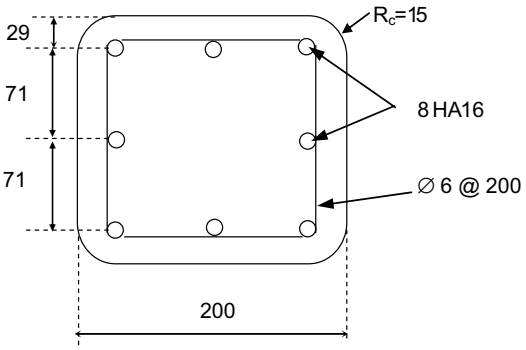

Fig. 5. Detail of reinforcement.

and the number of layers varies along the height. SC-PW-3C 1 was reinforced by carbon strips of 100 mm in width and 100 mm apart; it had three layers near the embedding and two at middle height. The same reinforcement ratio was used for SC-PW-3C 2, with 50 mm bands every 50 mm. Two 150 mm wide strips of three carbon layers were glued on specimen SC-PW-3C 3. Glass fibre was used for the last column. We carried out strength equivalence between 1 carbon layer and 3 glass layers. SC-PW-9G is thus reinforced in the same way and in the same ratio as SC-PW-3C 1 (Fig. 6).

The premature failure of the FRP reinforcement may be due to irregularities in the concrete [17,18]; this phenomenon is more pronounced for square sections. Even when the angles are rounded, the stress is still concentrated at the angles, so two layers of FRP is a minimum [19]. The angles were rounded to avoid FRP cracks due to local failure and stress concentration.

The columns and their footing were cast at the same time in order to ensure their perfect structural integrity. The concrete mix is given in Table 4.

The concrete compression tests are carried out on five 16×32 cm cores. It is therefore possible to determine the compressive strength of the concrete $fc = 31.5$ MPa $\pm$ 1.5 MPa.

2.3. Loading device

The loading device (Fig. 7) permits the application of a horizontal displacement to the top of the column. A constant compressive load is applied to the top of the column, representing the loads of the higher floors of buildings and the service loads. The horizontal loading must form a double curve; this involves identical moment at the embedding (foot and head) and a constant shear stress on the whole height of the column. It is applied to the middle of the column through an *L*-shaped steel framework. The horizontal part of the "*L*" is fixed on the column, with threaded rods passing through the holes in the upper column footing.

The load applied to the column must produce only horizontal displacement of the top of the column. The rotation

Table 4
Concrete mixture

Cement	350 kg/m^3
Water	190 kg/m^3
Gravel	950 kg/m^3
Sand	880 kg/m^3

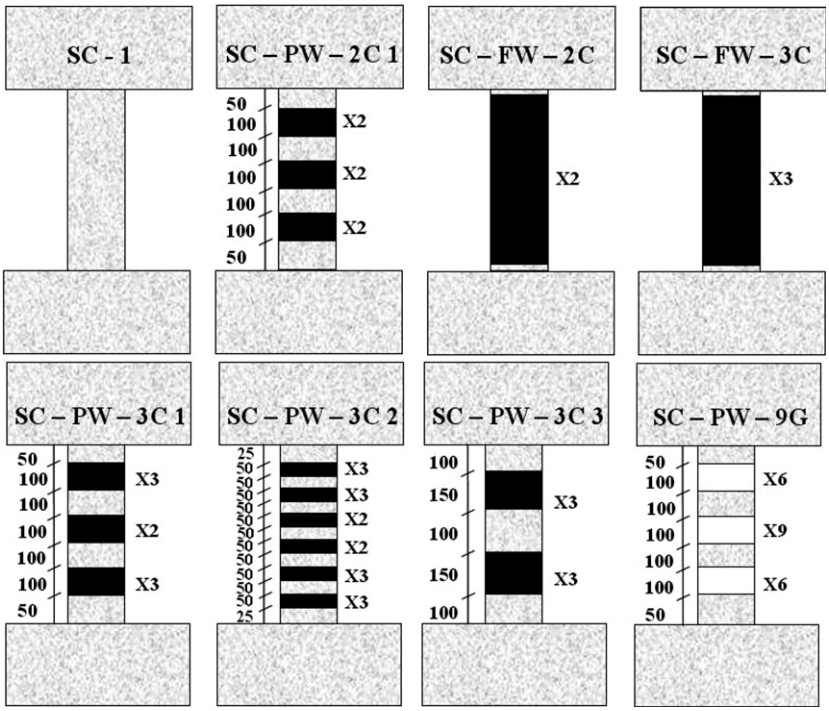

Fig. 6. Columns configurations.

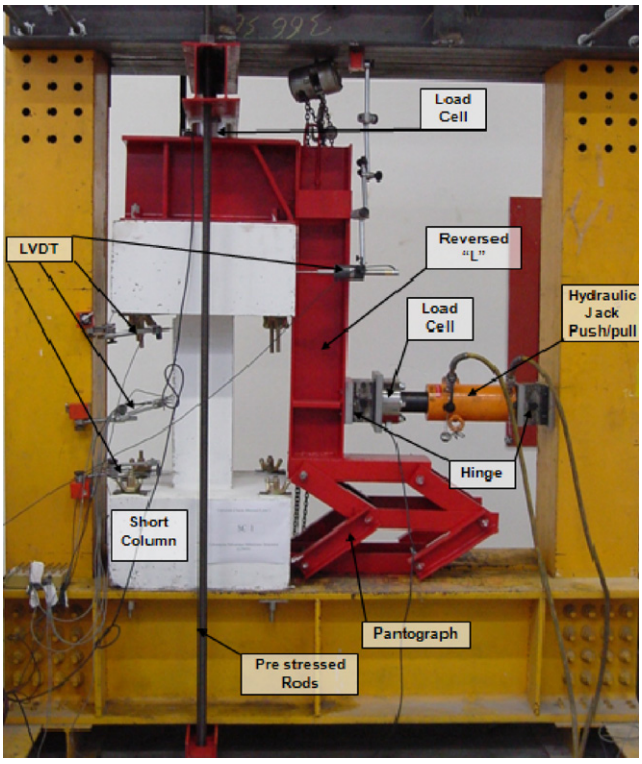

Fig. 7. Experimental device.

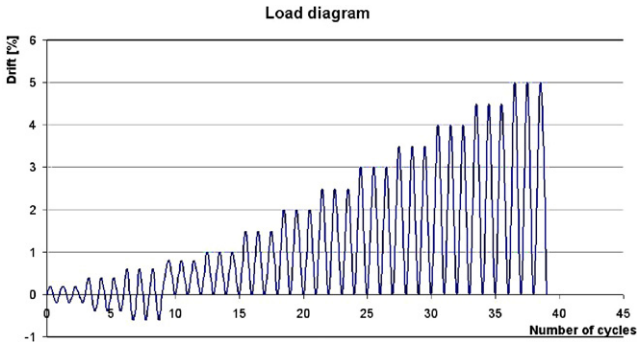

Fig. 8. Load diagram.

of the foundation must be limited. To do this, a pantograph is used. This double parallelogram allows only horizontal or vertical translations and prevents rotation.

The axial load is applied via prestressed rods (ϕ 26 mm, $F_{PEG} = 443$ kN, $F_{PRG} = 547$ kN). The column's head is mobile (in translation only), so the jack should be able to move in order to maintain a constant load. Despite being prestressed, the threaded rods retain a rotational capacity.

2.4. Loading diagram

The horizontal loading is controlled in displacement: three push-pull cycles are carried out each time in order to stabilise the hysteresis loops. Relative displacement (drift) noted R corresponds to the ratio displacement at the column head Δ (imposed) and height H. The drift values are $R = 0.2\%$; 0.4%; 0.6%; 0.8%; 1% and the displacements imposed after 1% are multiples of 1 (Fig. 8). The drift values were chosen because most failures of short columns found in the literature were obtained for a drift ranging between 0.5% and 1%, whereas for CFRP-strengthened columns they appeared for values of over 4%. For $R < 1\%$, closer cycles were used so as to have enough data for the unstrengthened column.

2.5. Instrumentation

The horizontal cyclic loading was applied quasi-statically, by a hydraulic jack with a capacity of 500 kN in compression and 170 kN in tension. A load cell with a tensile capacity of 500 kN in compression was placed between the L-shape and the jack. Vertical load was measured by a 1000 kN load cell.

Horizontal displacement at the top of the column was measured by an LVDT. Three other LVDT were placed on the column, and the one on the column base measured rotation. Steel and composite strains were measured with strain gauges (Fig. 9) bonded in various places. The acquisition frequency is 1 Hz.

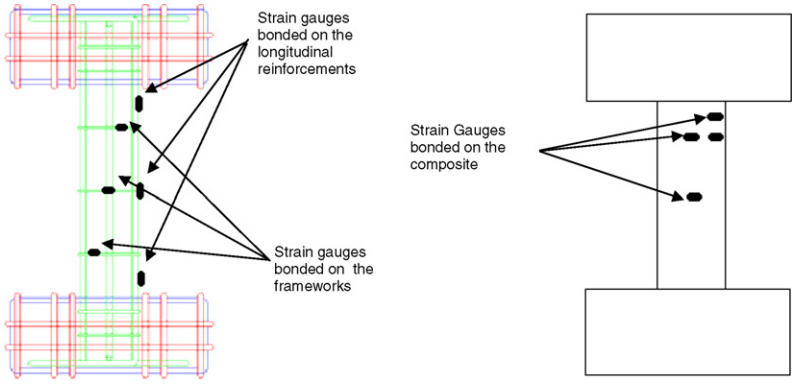

Fig. 9. Localisation of the strain gauges.

3. Results

3.1. Load and failure mode

Ultimate load is the first parameter of comparison. It allows the direct quantification of the effects of FRP reinforcement. The second parameter is failure mode. These results are presented in Table 5. The partially reinforced columns have a lower resistance than the fully confined ones.

The fully reinforced columns present bending failure, while for the partially reinforced ones it is mainly shearing failure. For a same cracking pattern the ultimate loads are almost identical, at all rates of reinforcement (Fig. 10). The ultimate load is doubled for the columns SC-PW-2C and 3C. The load variation between these two specimens is less than 1.5%, which corresponds to the measurement uncertainty. The load increase of the columns reinforced by bands varies from 65% to 70% for the bands of 100 and 150 mm. The column with bands spaced at 50 mm (SC-PW-3C 2) seem to have the least effective configuration, with a load-increase limited to 55% (relative to SC 1), although it was reinforced at the same rate of FRP as SC-PW-3C 1. Distributed cracking between bands occurred. This column is thus more susceptible to damage.

Table 5
Ultimate loads and associated failure mode

	Experimental results	
	Ultimate load (kN)	Failure mode
SC 1	128.30	Shear
SC-PW-2C	217.90	Shear
SC-FW-2C	256.60	Bending
SC-FW-3C	260.10	Bending
SC-PW-3C 1	211.56	Shear
SC-PW-3C 2	199.11	Shear
SC-PW-3C 3	218.66	Shear
SC-PW-9G	223.47	Shear

The column reinforced by glass fibre presents a load increase of close to 75%. The reinforcement design and its bonding configuration is strictly identical to the column SC-PW-3C 1.

To facilitate the analysis of the various reinforcement configurations, the load–displacement curves of the partially reinforced columns and of the non-reinforced columns were plotted together (Fig. 11). Then the same curve was plotted taking into consideration the reinforcement material (Fig. 12) and the bonding configuration (continuous or partial reinforcement) (Fig. 13); for these two parameters, the reinforced concrete column SC 1 and the partially reinforced column SC-PW-3C 1 were used. The latter column was chosen because it was strictly identical to column SC-PW-9G in terms of resistance and reinforcement configuration.

3.1.1. Influence of the width and spacing of the bands

A clear modification of column behaviour appears. The unstrengthened column SC-1 has elastic behaviour until failure. The break is brittle and does not allow the column to support any more loading. The reinforcement by bands of column SC-PW-2C (smallest quantity of bonded reinforcement), confers a greater strength and deformation capacity (respectively, +70% and +455%). So this reinforcement strategy is based on increased resistance and ductility (Fig. 2). The load–displacement diagram of column SC-PW-2C shows three stages (Fig. 10): a first, elastic stage, where the two curves (SC-1 and SC-PW-2C) are perfectly superimposed: the composite does not change column stiffness before the columns crack. After the cracking, the curve slope inflects. This stage corresponds to column damage. The degradation of the mechanical properties is due to the cracking of the concrete and to the rebars yielding. Increased displacement involves an increasingly diffuse cracking pattern. The reinforcements yield gradually. The third stage is a yielding stage which results from the total yielding of the reinforcement: the

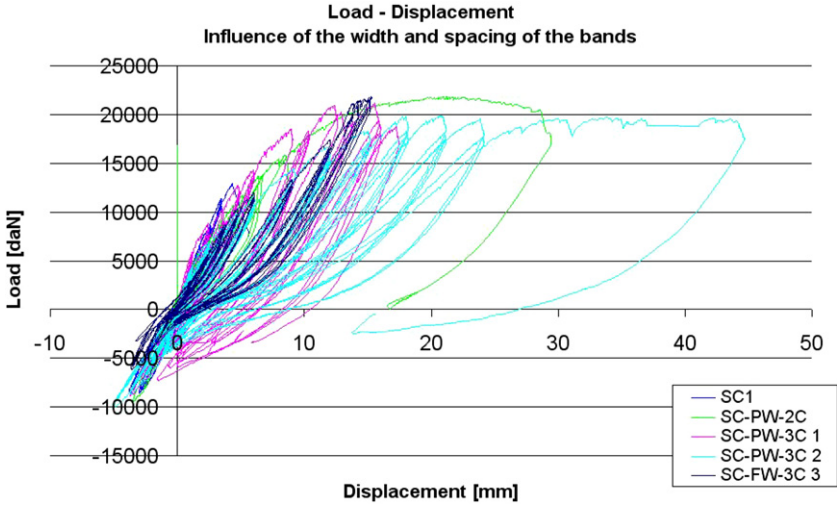

Fig. 10. Influence of the with and spacing of the bands – load/displacement curves.

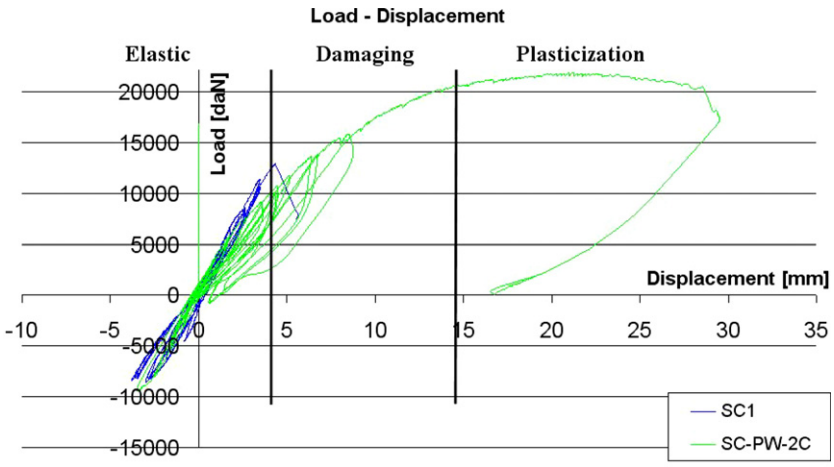

Fig. 11. Description of the three behaviour phases.

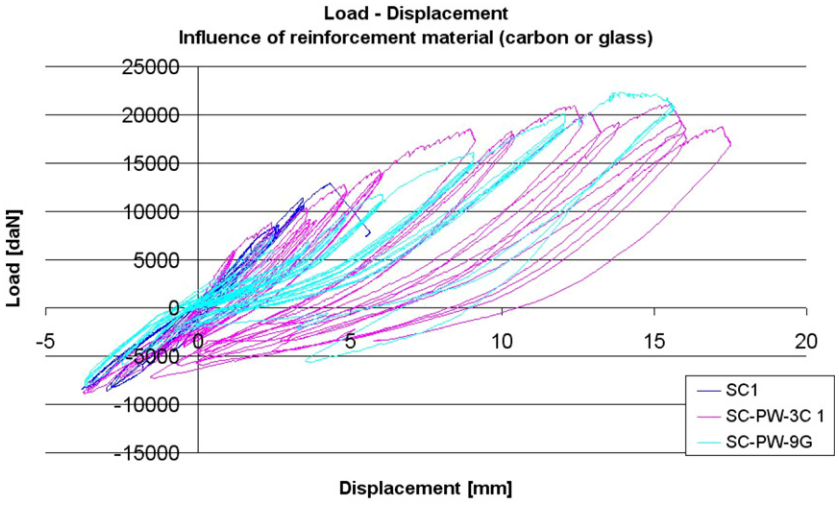

Fig. 12. Influence of the reinforcement material – load/displacement curves.

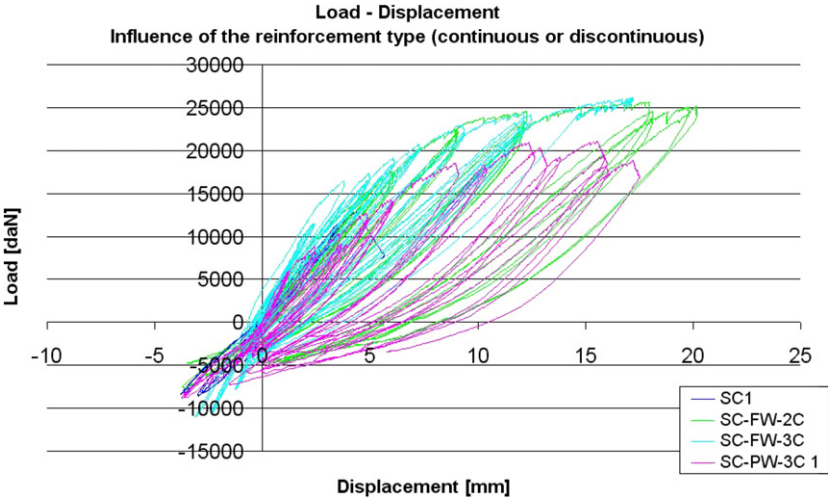

Fig. 13. Influence of the reinforcement type – load/displacement curves.

rupture of column SC-PW-2C occurred after the composite failure following stress concentration at the angles (which did not occur with the reinforced columns). Whatever the width and the spacing of the bands, the overall behaviour of the reinforced columns did not change.

3.1.2. Influence of reinforcement material (carbon or glass)

The observations previously made remain valid. The three stages of behaviour are identical to the previous case. The Young modulus for glass reinforcement is lower than that for carbon and column SC-PW-9G is slightly more flexible than the carbon one (for stiffness, see Table 6). So the yield stress changed, although ultimate resistance was equivalent.

3.1.3. Influence of the reinforcement type (continuous or discontinuous)

Column SC-FW-2C (reinforced with two continuous carbon sheets) presents a nearly identical behaviour to SC-PW-3C 1. It too presents three stages. However, the elastic stage continues to a load of 21.6 kN (an increase of 68%). After reaching the level of loading at which column SC-1 failed, the slope of the curve did not change: the initial stiffness is not affected by the FRP. The cracking of the concrete and its expansion are blocked by the composite. The prolongation of the first stage is made to the detriment of the second, and concrete damage is limited. During this second stage we observed multi-cracking of the columns between the bands in SC-PW-3C 1. The third stage was reached at loading levels higher than for column SC-PW-3C 1; this is explained by the fact that the CFRP confining pressure improves steel–concrete adherence. Because of the limitation of the tensile bars' slip, this is a better use of the reinforcements (yielding). At the end of the test, all columns reinforced by bands presented longitudinal cracks. These cracks occurred along the longitudinal rebars; the degradation of the steel–concrete interface is then obvious. Another phenomenon explaining the increase in resistance is that the concrete is well confined when the column is fully reinforced. The confined concrete can reach higher levels of resistance and deformation. The resistance increase of the confined concrete was evaluated at 15%. For the entirely reinforced column, energy dissipation is mainly performed by two plastic hinges in the embeddings, due to the yielding of the longitudinal reinforcements; this phenomenon was confirmed by the steel strain gauges. The behaviour of column SC-FW-3C is nearly identical to that of column SC-FW-2C.

Table 6
Calculations of the ductility coefficients

	Elastic displacement (mm)	Ultimate displacement (mm)	μ
SC 1	5.148	5.148	1.000
SC-PW-2C 1	7.826	28.389	3.628
SC-FW-2C	9.238	20.159	2.182
SC-FW-3C	3.758	17.173	4.570
SC-PW-3C 1	8.963	17.226	1.922
SC-PW-3C 2	18.017	44.090	2.447
SC-PW-3C 3	13.513	15.282	1.131
SC-PW-9G	13.593	15.640	1.151

3.2. Ductility

An earthquake imposes displacements on the columns and the walls. The aim of the design recommended by French and European regulations PS – 92 or EC 8 is to give the structure a certain freedom of displacement. This capacity of deformation must occur in the plastic range. A principle for reinforcement would thus be to allow the greatest possible ultimate displacement. Another means of evaluating this capacity is by calculating the ductility coefficient. Ductility refers to the capacity of a part to yield without breaking. Rupture occurs when a defect (crack or cavity) induced by the yield strains becomes critical and is propagated. Ductility is thus the aptitude of a structure to deform without breaking. If it does this well, it is known as ductile, if not it is known as brittle. The index of ductility is calculated in the following way:

$$\mu = \frac{\text{Ultimate displacement}}{\text{Elastic displacement}} = \frac{\Delta u}{\Delta e} \quad (1)$$

Reinforced concrete column SC 1 presents a coefficient of ductility μ equal to 1, a sign of brittle failure. The ductility of the CFRP reinforced columns, on the other hand, avoids the problem of brittle failure. The ductility coefficient of columns SC-PW-3C 3 and SC-PW-9G is equal to $\mu = 1.15$, so their failure is also regarded as brittle. Other columns too present ductile behaviour ($\mu > 2$). The most ductile column was one reinforced on its entire height by 3 layers of carbon sheet SC-FW-3C; its ductility is quite relative because it does not increase with a rise in the bending deformation of the column but by considerable rotation at the embeddings. The reinforcement caused a significant increase in displacement (×1.5–3.5). Ductility indices of 5 or 6, which occur in civil engineering, were not reached. Reinforcing short columns against seismic forces is, thus, complex. Regarding the possible strategy of reinforcement (Fig. 2), it would be necessary to choose a mixed strategy (ductility + load) since the gain in load is real while the gain in ductility is limited. It would also be necessary to study other indices such as stiffness and energetic capacity.

3.3. Stiffness

With the increase in displacement and in the number of cycles, the hysteretic loops tend to be inclined. This modification corresponds to a reduction in stiffness. This characteristic permits a quantification of the damage. Indeed, with the imposed boundary conditions, the stiffness can be evaluated by the following expression:

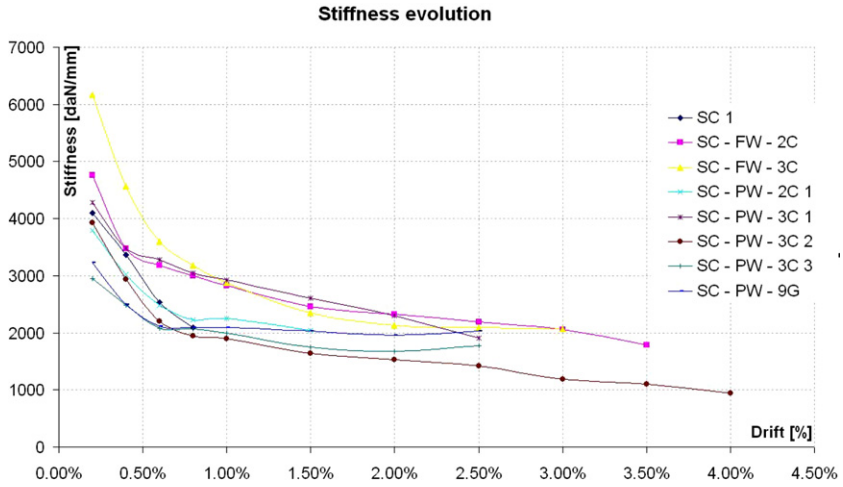

Fig. 14. Evolution of the stiffness according to imposed drift.

$$K = \frac{6 \cdot E \cdot I}{L^3} \quad (2)$$

E and I are respectively the elastic modulus and the inertia of the column and L is its length. At the time of damage, the mechanical properties of the materials are diminished. The cracking of the concrete reduces the structural integrity: this corresponds to a reduction in the inertia of the section. The variation in stiffness corresponds to the modification of the product of $E \times I$. Stiffness was calculated for the three cycles with the same drift, and an average was taken. Stiffness is always greater in the first cycle than the others. This is explained by the fact that the first cycle damages the materials (cracking of the concrete, steel yielding, and failure of the steel–concrete adherence). After this drift-specific damage, the column properties stabilise. Fig. 14 illustrates the progressive reduction in stiffness which renders a logarithmic curve. It is particularly marked for a 0.8% drift. This first stage corresponds to the behaviour of uncracked concrete columns. The load on the composite increases as the concrete degrades. This produces the second curve, in which degradation seems linear relative to drift. Beyond $R = 0.8\%$, the average degradation of the stiffness is 300 daN/mm for every 1% of additional drift, independent of the reinforcement rate and strategy, and of the material.

4. Energy analysis

The energetic properties were evaluated for the three cycles of each step of drift. The values in Tables 7 and 8 are the sums of the energy, elastic or dissipated, for the three cycles. A short program was used to automate the energetic calculations. The numeric method used is the calculation of integrals by the trapezoid method.

4.1. Elastic energy

4.1.1. Influence of the width and the spacing of the bands

During the first step of loading, to a drift equal to 0.8%, the composite contribution is null (Fig. 15). At this time the concrete column is elastic (see results of SC 1). Beyond $R = 0.8\%$, cracking starts and the composite starts to be solicited. From drift $R = 1\%$, column SC 1 is not represented because it was already broken. Over a drift value of 2%, there is no one particularly advantageous CFRP configuration. The columns have similar properties for all

Table 7
Elastic energy

Drift (%)	Elastic energy (J)							
	SC 1	SC-PW-2C	SC-FW-2C	SC-FW-3C	SC-PW-3C 2	SC-PW-3C 1	SC-PW-3C 3	SC-PW-9G
0.20	139.2	137.0	123.6	267.9	185.7	171.9	59.9	118.1
0.40	559.9	450.9	428.6	725.7	500.2	487.4	320.7	380.5
0.60	863.2	844.3	791.7	1538.6	891.2	830.1	596.1	601.2
0.80	538.5	523.9	1055.6	1232.6	452.2	535.0	581.0	501.2
1.00		733.7	1342.3	1637.9	768.3	755.4	778.7	719.4
1.50		1260.3	2402.7	2484.6	1275.0	1374.0	1144.1	1379.3
2.00			2819.6	3413.9	1776.6	1818.8	1858.0	2242.7
2.50			/	/	2295.5	1693.5	3141.1	2499.8
3.00			3329.3	6510.7	2644.6			
4.00			3397.3		2695.1			

Table 8
Calculations of dissipated energies

Drift (%)	Dissipated energy (J)							
	SC 1	SC-PW-2C	SC-FW-2C	SC-FW-3C	SC-PW-3C 1	SC-PW-3C 2	SC-PW-3C 3	SC-PW-9G
0.20	19.9	36.7	22.1	60.7	46.4	78.7	16.7	42.4
0.40	341.5	156.2	6.2	62.1	192.7	88.9	60.7	151.1
0.60	134.7	334.2	55.2	218.4	271.9	139.7	267.3	116.1
0.80	74.3	125.0	76.5	193.2	209.2	89.4	150.4	81.3
1.00		277.3	134.1	276.9	215.5	189.7	193.9	115.7
1.50		585.0	285.9	603.5	656.5	408.6	250.4	290.0
2.00			575.2	1091.5	1133.2	566.2	461.5	409.9
2.50			/	/	1266.6	882.1	583.8	922.5
3.00			939.3	1168.7		1334.2		
4.00			1037.6			1686.8		

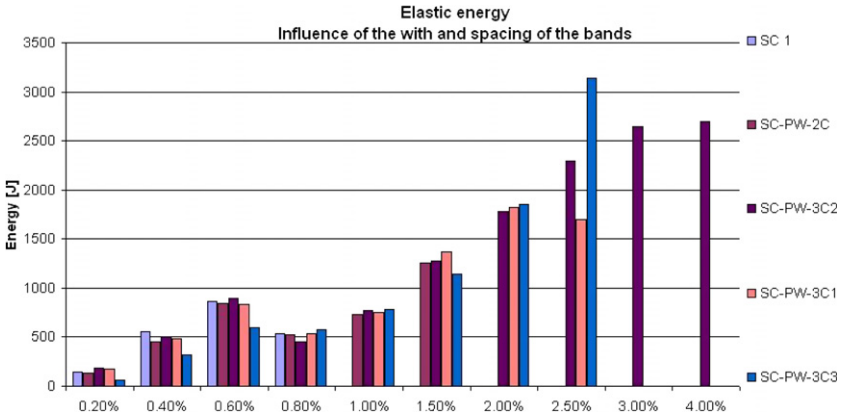

Fig. 15. Influence of the with and spacing of the bands – elastic energy.

values of band spacing and width. From $R = 2.5\%$, the 150 mm strips at 100 mm spacing seem to be the best solution, as suggested by the failure of SC-PW-2C due to premature rupture of the composite. A decrease in elastic energy capacity in SC-PW-3C1 (−7%) was observed as displacement increased. This is a sign of irreversible damage. The capacities of columns SC-PW-3C 2 and 3C 3, on the other hand, increased by 30% and 70%, respectively. Beyond $R = 2.5\%$ the test was over for all the columns except SC-PW-3C 2, where, however, asymptote had appeared – a sign of imminent severe damage. Its elastic capacity was nevertheless lower than that of SC-PW-3C 3 for lower displacements.

4.1.2. The influence of material reinforcement (carbon or glass)

At drift values of less than 1.5% it was difficult to determine which material was best (Fig. 16), as cracking had not yet begun. The results were quite similar. SC-PW-3C1 had lower elastic properties than the glass column, starting

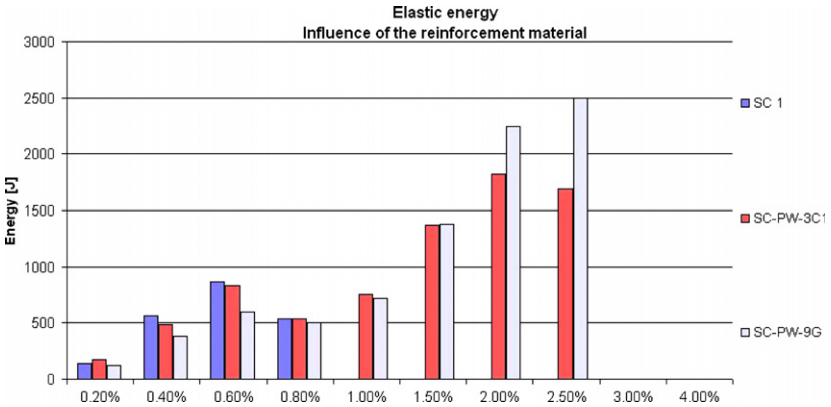

Fig. 16. Influence of the reinforcement material – elastic energy.

from $R = 2\%$ (-19% with $R = 2\%$ and -32% with $R = 2.5\%$). For the next level of displacement, the elastic reserve started to fall, announcing failure. However, displacement of the column reinforced with glass still increased, by 63% and by 11.5% for $R = 2.00\%$ and 2.5%, but the benefit is not so great when cracking is taken into account. The glass material thus seems more suitable. These first conclusions are subject to confirmation by the dissipated energy analysis.

4.1.3. Influence of the reinforcement type (continuous or discontinuous)

The analysis of the reinforcement type (continuous or discontinuous) is less complicated, and easier to comment. The completely reinforced columns have definitely higher elastic properties than the column reinforced by bands (Fig. 17). Even for drift lower than 1%, the effects of total confinement can be noted. The explanation lies in the fact that total confinement blocks any cracking of the concrete, reduces the stress of stirrups and concentrates the efforts in the embeddings. Rigid body displacement was observed, particularly significant for the higher rate of confinement.

Our conclusions regarding the elastic energy aspect await confirmation from the study of dissipative behaviour. The new codes recommend dissipation of energy by cracking and multi-yielding rather than by storage in elastic form. Elements thus designed have a brittle failure mode.

4.2. Dissipated energy

4.2.1. Influence of the width and the spacing of the bands

During the first loading cycles, the SC 1 column cracks were macroscopic and brittle, unlike the reinforced columns where they remained microscopic. Thus SC1 dissipated more energy (Fig. 18). From $R = 0.60\%$, the stiffness fell, the slope of the hysteretic loop involved weakened energy capacities (-60% then -45% for the drift factor of 0.60% and 0.80%). This signalled the imminent failure which occurred at $R = 0.96\%$. The dissipated energy of SC-PW-2C was higher than that of all the other reinforced columns. It should be noted that this column was reinforced with the lowest rate of FRP. It thus allowed concrete cracking (diffuse between the bands), as well as the yielding of framework and longitudinal reinforcement (although a composite strip was found to be broken at the end of the test). Considering all these parameters, SC-PW-2C was the most dissipative to $R = 1.5\%$. At this level the damage is such that failure is imminent. However, from this stage of drift, SC-PW-3C 1 was the best solution. The FRP was implemented with

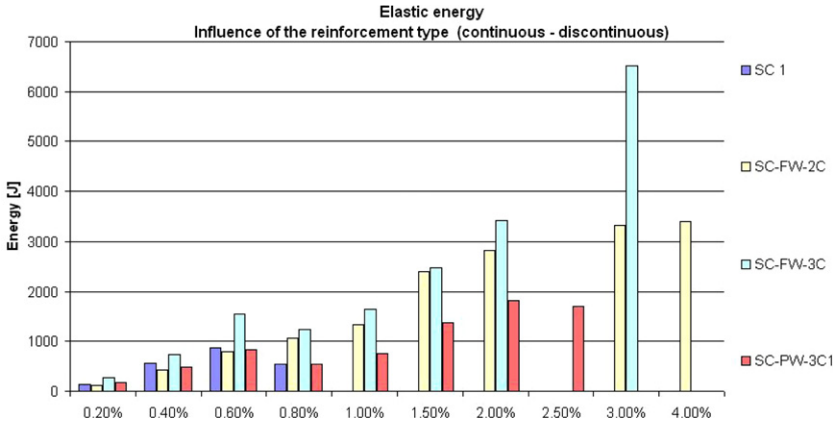

Fig. 17. Influence of the reinforcement type – elastic energy.

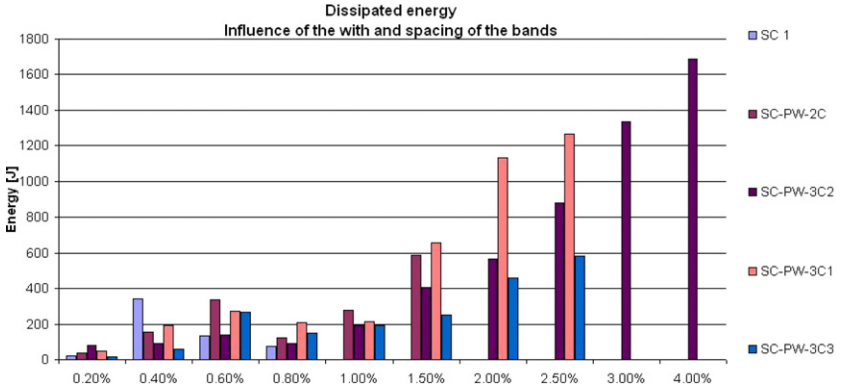

Fig. 18. Influence of the width and spacing of the bands – plastic energy.

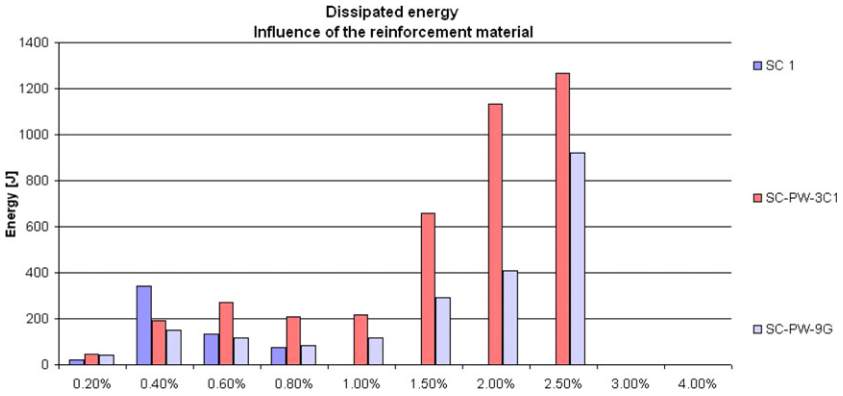

Fig. 19. Influence of the reinforcement material – plastic energy.

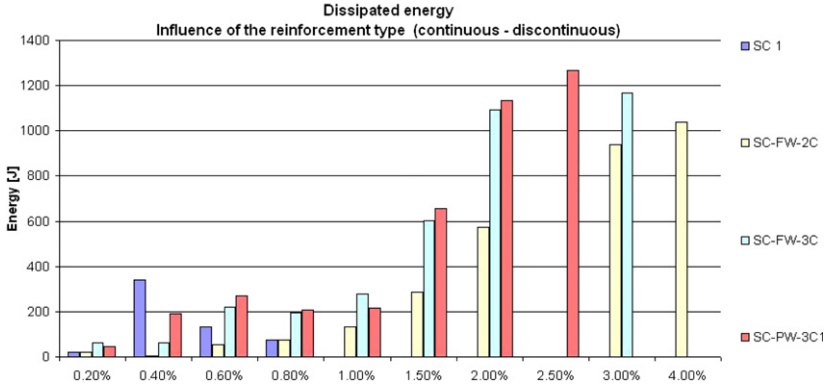

Fig. 20. Influence of the reinforcement type – plastic energy.

the same configuration, but with one more layer of CFRP (foot and head). This configuration is 100% stronger than the bands of 150 mm for drifts of 1.50%, 2.00% and 2.50%. The second-best configuration was the weak strips (SC-PW-3C 2), which had exactly the same reinforcement rate as SC-PW-3C 1. The energy dissipation of SC-PW-3C 1 increased very slowly, while that of column SC-PW-3C 2 increased strongly. This CFRP configuration permits the attainment of drift as high as 4%. This is thus the strongest configuration. The principal reason is the multi-diffuse cracking between the bands, which permits considerable energy dissipation.

4.2.2. Influence of the reinforcement material (carbon or glass)

During the elastic analysis, glass material appeared to be a good solution. The plastic study best adapted to the seismic problem gave a different picture. The choice of GFRP was made based on the ultimate strain of the laminate. It is equal to 1.8%, as opposed to 0.85% for CFRP. This value of ultimate strain was previously thought to be favourable. GFRP should have allowed more concrete cracking, more steel–concrete slip and more local yielding. Consequently the dissipated energy should have been higher than with the CFRP solution. This is not, however, observed in Fig. 18. The results are not satisfactory for the glass reinforced column which dissipates less, as of the first loading cycles. As displacements increase so does the difference in energy dissipation (-8.5% with $R = 0.20\%$, -22% with $R = 0.40\%$, -57% with $R = 0.60\%$, -61% with $R = 0.80\%$, -46% with $R = 1.00\%$, -56% with $R = 1.50\%$, -64% with $R = 2.00\%$ and -27% with $R = 2.50\%$). Moreover, these conclusions confirm the fact that elastic energy is more significant; indeed, reinforcement caused an increase in the stiffness of the column (after cracking), which, combined with the column's low resistance to damage, led to the conclusion that GFRP was less effective than CFRP. Yet these columns are strictly equivalent in term of resistance. Strength equivalence was carried out in order to avoid any risk of local tensile failure as observed in SC-PW-2C (see Fig. 19).

4.2.3. Influence of the reinforcement type (continuous or discontinuous)

Remarks made previously for small displacements remain valid. FRP material bridged the few cracks which appeared and energy dissipation was thus weak. For greater displacements, the number of strips appeared to be important. The least reinforced column dissipated less energy (Fig. 20). This is probably due to the fact that the behaviour of the columns was completely different. The column reinforced by three sheets is stiffer and deformation

by rotation around the two footings was observed. Energy dissipation for this column is by localised yielding (foot and head), and by cracking and crushing of the concrete of the soles and the ends of the columns (local over-compressive loading). Equivalent or higher performances were reached with reinforcement by bands. This configuration is advantageous as it requires less reinforcement: with over 50% less fabric, energy dissipation was increased by +10% and +5%, respectively, for drifts of 1.5% and 2.0%. Moreover, up to a drift level of 2.5%, SC-PW-3C 1 dissipated more energy than the completely reinforced columns (10% more compared to SC-FW-3C and 26% compared to SC-FW-2C). Thus the choice of reinforcement strategy is clearly discontinuous confinement.

5. Conclusions

FRP reinforcement completely changed the failure mode of the columns. For the two entirely wrapped columns brittle shear failure changed to ductile bending failure, while in the strip-reinforced column failure was due to shear-bending. The strategy of FRP reinforcement in this study involves the increase of both resistance and ductility.

Reinforcement by strips provides a more advantageous dissipative behaviour than the fully wrapped columns. This is due to the ductility gained through the following two mechanisms:

- Damage to the concrete by cracking between the FRP strips.
- Yielding of the reinforcements in all column sections.

For the columns which were fully wrapped in FRP, ductility was increased, mainly due to transfer to the embeddings, creating a hinge by advanced yielding of the longitudinal reinforcements. The FRP reinforcement allowed rotation in the embedding sections, without buckling of the compressed reinforcements, although they greatly exceeded their elastic limit. Even for the short columns, the central section was less solicited that the embedding sections. So it seemed that using a different thickness of reinforcement would be advantageous.

Composite material reinforcement endowed the short columns with ductile behaviour, although the columns did not contain the necessary transversal reinforcement ratio. Care must be taken not to oversize the FRP reinforcement, as this results in a transfer of effort to the nodes. Finally, the strategy of reinforcement must be total and non-local.

Acknowledgements

The authors thank the GTM Construction company (subsidiary company of Vinci) for its financial support, the use of its reinforcement process of wet laid-up composite ROCC®, and also for authorisation to use their results.

References

[1] Walker RA, Karbhari VM. Durability based design of FRP jackets for seismic retrofit. Compos Struct 2007;80(4):553–68.
[2] Taljsten B. Strengthening of beams by plates bonding. J Mater Civil Eng 1997;9(4):206–12.
[3] Paulay T. seismic design strategies for ductile reinforced concrete structural wall. In: Proceedings of international conference on buildings with load bearing concrete walls in seismic zones, Paris; 1991. p. 234–44.
[4] Cheng CT, Yang JC, Yeh YK, Chen SE. Seismic performance of repaired hollow-bridge piers. Construction and Building Materials, vol. 17. Elsevier Science Ltd.; 2003. p. 339–51.
[5] Fukuyama J. The Japan Building Disaster Prevention Association. Seismic retrofit design and guidelines for existing RC buildings and steel encased RC buildings using continuous fiber reinforced materials. The Japan Building Disaster Prevention Association, Ministry of Construction; 1999. p. 45–56.
[6] Seible F, Preistley MJN, Hegermier GA, Innamorato D. Seismic retrofit of RC columns with continuous carbon fiber jackets. J Compos Construct, ASCE 1997;1(2):52–62.
[7] Teng JG, Chen JF, Smith ST, Lam L. FRP strengthened RC structures. John Wiley and Sons; 2002 [Chapters 1, 6 and 7].
[8] Maekawa K, An X. Shear failure and ductility of RC columns after yielding of main reinforcement. Engineering Fracture Mechanics, vol. 65. Elsevier Science Ltd; 2000. p. 335–68.
[9] Minowa C, Ogawa N, Hayashida T, Kogoma I, Okada T. Dynamic and static collapse tests of reinforced-concrete columns. Nuclear Engineering and Design, vol. 156. Elsevier Science Ltd; 1995. p. 269–76.
[10] Takahashi A, Tago S, Ilki A, Okada T. Seismic Capacity evaluation of existing reinforced concrete building in Turkey, effect of retrofit. In: Proceedings of 13th world conference on earthquake engineering, Canada: Vancouver, 1–6 August 2004. p. 455–63.
[11] Baouche N, Crainic L. Study of the behaviour of short columns under seismic loading for improving the earthquake resistant regulation codes RPA99. In: Proceedings of third international conference CONMAT, 2005. p. 234–40.
[12] Ilki A, Peker O, Karamuk E, Kumbasar N. External confinement of low strength britle reinforced concrete short columns. In: Proceedings of international symposium on confined concrete, Changsa, Chine, 12–14 June 2004.
[13] Galal K, Arafa A, Ghobarah A. Retrofit of RC square short columns. Engineering Structures, vol. 27. Elsevier Science Ltd.; 2005.
[14] Xiao Y, Wu H, Martin GR. Prefabricated composite jacketing of RC columns for enhanced shear strength. J Struct Eng, ASCE 1999;125(3):255–64.
[15] Eurocode 8, Design provisions for earthquake resistance of structures, AFNOR – 2000. XP ENV 1998-1-1, XP ENV 1998-1-2, ENV 1998-1-3.
[16] AFNOR, French building seismic design code PS 92 NF P 06-013, published in French; 1995.
[17] Lam L, Teng JG. Design-oriented stress–strain model for FRP-confined concrete. Construction and Building Materials, vol. 17. Elsevier Science Ltd.; 2003.
[18] Ricles JM, Yang HS, Priestley MJN. Modeling nonductile RC columns for seismic analysis of bridges. J Struct Eng, ASCE 1998;124(4):415–25.
[19] Mirmiran A, Shahawy M, Samaan M, El Echary H. Effect of column parameters on FRP confined concrete. J Compos Constr, ASCE 1998;2(4):175–85.